Aerodynamic Analysis of Helicopter Rotor using a Time-Domain Panel Method

Seawook Lee[1], Leesang Cho[2] and Jin-Soo Cho[3]

Summary

Computational methods based on the solution of the flow model are widely used for the analysis of low-speed, inviscid, attached-flow problems. Most of such methods are based on the implementation of the internal Dirichlet boundary condition. In this paper, the time-domain panel method uses the piecewise constant source and doublet singularities. The present method utilizes the time-stepping loop to simulate the unsteady motion of the rotary wing blade for the KHP. The wake geometry is calculated as part of the solution with no special treatment. To validate the results of aerodynamic characteristics, the typical blade was chosen such as, Caradonna-Tung blade and present results were compared with the experimental data and the other numerical results in the single blade condition and two blade condition. This isolated rotor blade model consisted of a two bladed rotor with untwisted, rectangular planform blade. Computed flow-field solutions were presented for various section of the blade in the hovering mode.

keywords: Time-domain panel method, Aerodynamic analysis, Rotary-wing, Free wake

Introduction

Currently, most nations have used great amount of their rotary wing aircraft in their military and industrial fields. The research on the aerodynamic characteristics of the rotary wing aircraft has been performed broadly. Although there were great amount of efforts that have developed the rotary wing aircraft, only few countries have their own rotary wing aircraft and design technology. Compared to fixed wing aircraft, the rotary wing aircraft has highly complex aerodynamic characteristics. Therefore, a large amount of both experimental tests and numerical analyses must be performed with numerous aerodynamic considerations.

The main rotor normally has many problems with complicated aerodynamic characteristics. The main rotor of the rotary wing aircraft generates not only the lift but also the thrust. The wake generated by the blade has an influence on the following blade and the strong tip vortices trails into the rotor wake. In the process of conceptual design, the numerous aerodynamic characteristics must be ana-

[1]Department of Mechanical Engineering, Hanyang University, Seoul, Korea. (Tel: +82-2-2220-1716; E-mail: mplsw@hanyang.ac.kr)

[2]Department of Mechanical Engineering, Hanyang University, Seoul, Korea. (Tel: +82-2-2220-1716; E-mail: ppome815@hanyang.ac.kr)

[3]School of Mechanical Engineering, Hanyang University, Seoul, Korea. (Tel: +82-2-2220-0429; E-mail: jscho@hanyang.ac.kr)

lyzed. Recently, the Computational Fluid Dynamics (CFD) techniques have been developed to solve various types of aerodynamic problems of the rotary wing aircraft. The CFD technology has been known as one of the powerful solutions in order to obtain the aerodynamic characteristics. However, the amount of computing resources and computing time still remain as the primary demerits in the CFD technology. To alleviate this problem, huge computing abilities beyond current computers is required. Therefore, a time-domain panel method is used for the aerodynamic analysis of the rotary wing aircraft for KHP. Time-domain panel method has strengths in both sides of little computing time and less computing resources.

Numerical Method

Formulation

The flow is assumed to be invicid, irrotational, and incompressible over the 3-dimensional shape and flow-field. Hence, a velocity potential $\Phi(x,y,z)$ can be defined, and continuity equation becomes Laplace's equation:

$$\nabla^2 \Phi = 0, \quad \overrightarrow{V} = \nabla\Phi \tag{1}$$

The general solution to Eq. (1) can be constructed, based on Green's identity, by a sum of source σ and dipole μ distributions on all of the known boundaries.

$$
\begin{aligned}
\Phi(P) = &-\frac{1}{4\pi} \iint_{body} \sigma\frac{1}{r} - \mu\frac{\partial}{\partial n}\left(\frac{1}{r}\right) dS \\
&+ \frac{1}{4\pi} \iint_{wake} \mu\frac{\partial}{\partial n}\left(\frac{1}{r}\right) dS + \Phi_\infty(P)
\end{aligned} \tag{2}
$$

To impose the Dirichlet boundary condition on the surface, the perturbation potential has to be specified everywhere on the body. If for an enclose body $\partial\Phi/\partial n = 0$, then the potential inside the body will not change. Thus, Eq. (2) becomes as follow.

$$
\begin{aligned}
\Phi(P) = &-\frac{1}{4\pi} \iint_{body} \sigma\frac{1}{r}dS + \frac{1}{4\pi} \iint_{body} \mu\frac{\partial}{\partial n}\left(\frac{1}{r}\right) dS \\
&+ \frac{1}{4\pi} \iint_{wake} \mu\frac{\partial}{\partial n}\left(\frac{1}{r}\right) dS = 0
\end{aligned} \tag{3}
$$

The unsteady motion are expressed by the Neumann problem on the surface of object due to no time-term in the Eq. (1)

$$\frac{\partial\Phi}{\partial n} = (V_O + v_{rel} + \Omega \times r) \cdot n = 0 \tag{4}$$

v_{rel} is the relative velocity on the body fixed coordinate and r is indicated as a position of panel control point.

2.2 Flight path and rotational information

As the shown Figure 1, (X, Y, Z) is determined as a inertial coordinate system, and (x, y, z) is considered as a body fixed coordinate. Therefore, the path of origin R and rotational information Θ can be combined with forwarding mode and vibration mode. Then this is expressed as below.

$$R_o(t) = -Q_\infty t + A \sin(\omega t - v)$$
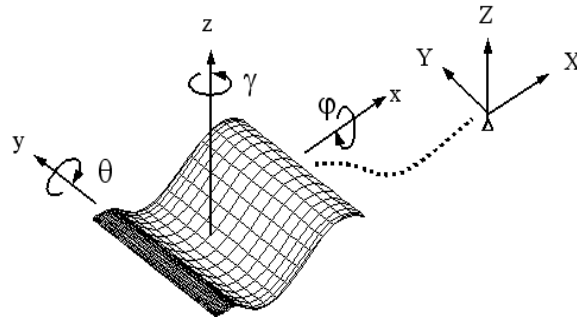$$\Theta(t) = -\zeta t + A \sin(\omega t - v) \tag{5}$$

Figure 1: Inertial and body coordinates used to describe the motion of the body

Now, the velocity V_o and angular velocity Ω can be written as the Eq. (6)

$$V_o(t) = -Q_\infty + A\omega \cos(\omega t - v)$$
$$\Omega(t) = -\zeta + A\omega \cos(\omega t - v) \tag{6}$$

At this point, free flow velocity, constant angular velocity, amplitude of vibration, frequency, and angle of delay are shown as Q_∞, ζ, A, ω, and v respectively.

To estimate the transformation of coordinate, the equation of transformation was shown as below.

$$\begin{pmatrix} x \\ y \\ z \end{pmatrix} = \begin{pmatrix} 1 & 0 & 0 \\ 0 & \cos\phi(t) & \sin\phi(t) \\ 0 & -\sin\phi(t) & \cos\phi(t) \end{pmatrix} \begin{pmatrix} \cos\theta(t) & 0 & -\sin\theta(t) \\ 0 & 1 & 0 \\ \sin\theta(t) & 0 & \cos\theta(t) \end{pmatrix}$$
$$\begin{pmatrix} \cos\psi(t) & \sin\psi(t) & 0 \\ -\sin\psi(t) & \cos\psi(t) & 0 \\ 0 & 0 & 1 \end{pmatrix} \begin{pmatrix} X - X_0 \\ Y - Y_0 \\ Z - Z_0 \end{pmatrix} \tag{7}$$

Wake grid generation

To sophisticated unsteady motion at the trailing edge or entire flow, the wake that flows from separation point which is determined by user is created by addition

of wake panels at each time interval Δt. The strengths of doublet at the wake-panel is computed with Morino Kutta condition each time and their strengths would be maintained along the time by the determination of Helmholtz.

$$\Phi_{wake} = \Phi_{upper} - \Phi_{lower} \tag{8}$$

In this paper, the new strength of wake was determined by the average value of the previous strength of wake as given in Eq. (9). Hence, The Kutta condition can be applied more accurately and the pressure gradient can be minimized.

$$\Phi_{average} = \frac{\Phi_{wake}(t) + \Phi_{wake}(t - \Delta t)}{2} \tag{9}$$

Strength of source and doublet

It is possible to set the doublet strength or the source strength to zero, in a manner similar to the thick and thin airfoil cases. A frequently followed choice for panel methods is to set the value of the source distribution equal to the local kinematic velocity. In order to justify this, observe the Neumann boundary condition, which states that on the solid boundary,

$$\frac{\partial \Phi}{\partial n} = (V_o + v_{rel} + \Omega \times r) \cdot n \tag{10}$$

However, Eq. (1) states that the jump in the local normal velocity component is as follow.

$$-\sigma = \frac{\partial \Phi}{\partial n} - \frac{\partial \Phi_i}{\partial n} \tag{11}$$

Since $\Phi_i = 0$ then also $\partial \Phi_i / \partial n = 0$ on the solid boundary S_B. Consequently, the source strength is became as below.

$$\sigma = -n \cdot (V_o + v_{rel} + \Omega \times r) \tag{12}$$

To obtain the strength of doublet, fixed strength of source is discretized to the equation as follow.

$$[A_{NN}] \begin{bmatrix} \mu_1 \\ \mu_2 \\ \vdots \\ \mu_N \end{bmatrix} = [B_{NN}] \begin{pmatrix} \sigma_1 \\ \sigma_2 \\ \vdots \\ \sigma_N \end{pmatrix} + [C_{NN}] \begin{pmatrix} \mu_{w1} \\ \mu_{w2} \\ \vdots \\ \mu_{wM} \end{pmatrix} \tag{13}$$

On the above equation, N and M mean the number of total panel for the object, the number of wake panel respectively.

Calculation of velocity

The tangential velocity and the perturbation velocity are obtained at each panel as follow.

$$v_l = \frac{\partial \mu}{\partial l}, \quad v_m = \frac{\partial \mu}{\partial m} \tag{14}$$

The perturbation velocity of normal direction is shown as below.

$$v_n = -\sigma \tag{15}$$

Normally, the perturbation velocity on the tangential direction is obtained using the central difference method, can be obtained by Eq. (16)

$$v_l = \frac{\partial \mu}{\partial l} = \frac{1}{2\Delta l}(\mu_{l+1} - \mu_{l-1}), \quad v_m = \frac{\partial \mu}{\partial m} = \frac{1}{2\Delta m}(\mu_{m+1} - \mu_{m-1}) \tag{16}$$

However, due to the arbitrary shape, it is not useful to calculate with the difference method. In this paper, the VSAERO's [7] polynomial interpolation which has been used in the commercial panel code broadly was adopted to obtain the tangential velocity and the sum of the perturbation velocity plus local kinematic velocity which is the local fluid velocity as given in Eq. (17)

$$Q_k = V_{kine} \cdot (l, m, n)_k + (v_l, v_n, v_m)_k \tag{17}$$

Where $(l, m, n)_k$ are the local tangential and normal directions and the components of V_{kine} in these directions are obtained and V_{kine} is the magnitude of the kinematic velocity as follow.

$$V_{kine} = -(V_o + v_{rel} + \Omega \times r) \tag{18}$$

Calculation of pressure

The local perturbation velocity is $(v_l, v_n, v_m) = (\partial \Phi/\partial l, \partial \Phi/\partial m, \partial \Phi/\partial n)$ and of course the normal velocity component on the solid body is zero. The pressure coefficient can now be carried out for each panel as follow.

$$C_P = \frac{p - p_{kine}}{\frac{1}{2}\rho v_{kine}^2} 1 - \frac{Q^2}{V_{kine}^2} - \frac{2}{V_{kine}^2}\frac{\partial \Phi}{\partial t} \tag{19}$$

Wake rollup

The local velocity is related with the motion of the object. The wake rollup at each time step can be performed and each vortex of the wake both trailing edge and separated will move with the local velocity $(u, v, w)_l$ by the amount.

$$(u, v, w,)_l = (u, v, w,)_{l,body} + (u, v, w,)_{l,wake} \tag{20}$$

$$(\Delta X, \Delta Y, \Delta Z)_l = (u, v, w,)_l \cdot \Delta t \tag{21}$$

$$\begin{bmatrix} X \\ Y \\ Z \end{bmatrix}_l = \begin{bmatrix} X \\ Y \\ Z \end{bmatrix}_l + \begin{pmatrix} \Delta X \\ \Delta Y \\ \Delta Z \end{pmatrix}_l \tag{22}$$

Results

Validation

The developed code is three-dimensional. To validate this code with the result of two-dimensional code and theory, the blade is composed with aspect ratio = 1000, NACA 0012, AOA=8.3, and the total number of panel is 80×11. It was clearly satisfied with the Moran's theoretic result [2] and 2-D vortex panel method's results of the distribution of pressure coefficient that is from the center of span to the chord line. However, the minimum pressure coefficient was little bit low on the leading edge than the other results. This problem can be modified through that rearranged the distributions of the panels on the leading edge elaborately.

Generally, many of rotary wing aircrafts are adopted with sweep blade for improved aerodynamic characteristic of their main rotor. For example, UH-60a has been adopted sweep angle at the part of tip blade. However, it is quite not easy to predict to any aerodynamic characteristic when the blowing cross flow affects and high angle-of-attack due to a serious distortion of wake. To validate this case, the blade which composed with NACA 0012, taper ratio=0.5, aspect ratio=4.8, and AOA=10 degree to sweep blade is choose to calculate. The pressure distributions at the point of 10% span are shown in the Fig 3. It shows good agreements with the results of Hess [6]
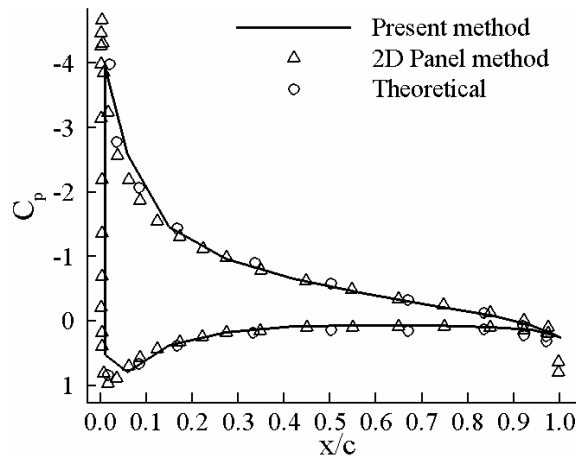

Figure 2: Pressure distribution of NACA 0012 at the AOA=8.3

Hovering flight

The one-blade which is composed NACA 0012 airfoil, R/c=6 was taken to compute the aerodynamic characteristics in the hovering flight. Under the consideration that the aerodynamic load of one-blade is not much different from two-blades, the shape of wake was computed after the rotor blade was rotated 4 times. Fig 4. shows that the wake geometry has much more tendencies to diffuse in the radial
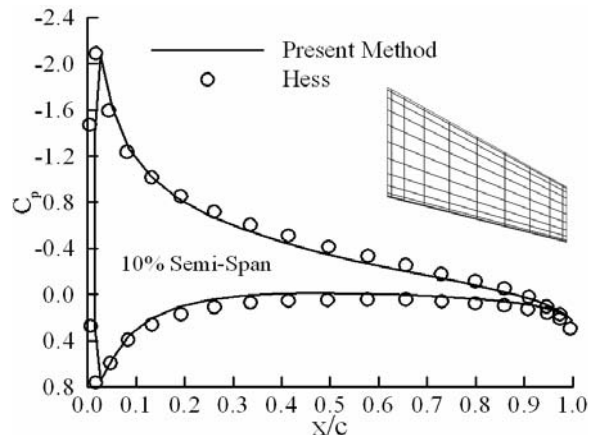
Figure 3: Pressure distribution of the thin swept blade

direction and the rising tornado shape of wake came out from the centre of rotor. It was observed that the outer part of the sheet moves faster than the inner part, with the result that the sheet becomes more inclined to the rotor plane, and that the outer part of the sheet moves faster than the tip vortex. The pressure distribution at the region of blade tip ($r/R_{rotor} = 0.8$) is shown in the Fig. 5. This result is approximately closed to the experimental result. The error between this numerical result and the experimental result was occurred because of array of panels and the number of panels. Of course, it is quite one of the serious reason that the experimental results are taken in case of two blades to compare with numerical result.

The aerodynamics analysis of two blades was performed. The wake geometry in this case was computed and shown in the fig. 6. The blade was composed NACA 0012 airfoil, AOA=8, and R/c=6. The pressure coefficient was calculated at the section of r/R=0.6 under 2500rpm ($M_{tip} = 0.877$) as in the fig. 7. The results of aerodynamic characteristics which is by this method are validated against the experimental results of Caradonna and Tung [4] on a constant chord, untwisted, two bladed rotor. Fig. 7. shows good agreements comparison between two of them.

Conclusions

Time-domain panel method was used to develop the 3-D code for a rotary wing aircraft. The present method was assumed incompressible, irrotational flow, and using the source-doublet. The present method utilizes the time-stepping loop to simulate the unsteady motion of the rotary wing blade for the KHP. The wake is calculated as part of the solution with no special treatment. To validate the developed code, the aerodynamic analysis was taken for the 2-D airfoil blade which has a taper ratio and sweep angle. The slow starting method was adopted in order to apply the inflow model which can alleviate the problems of a bird strike for the
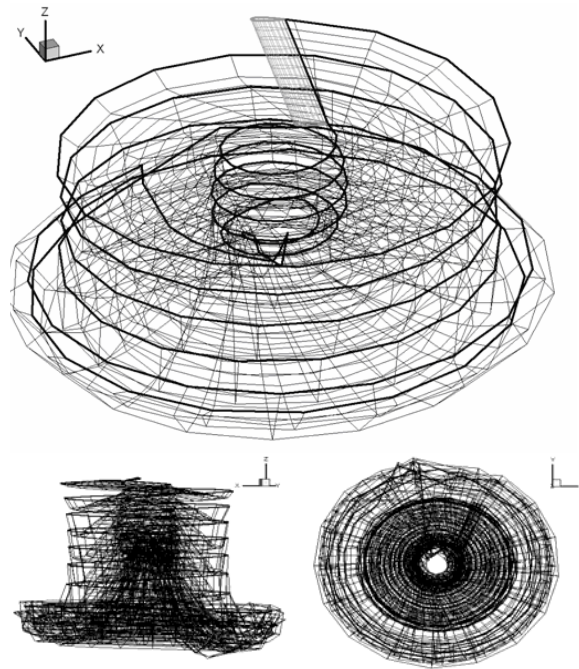
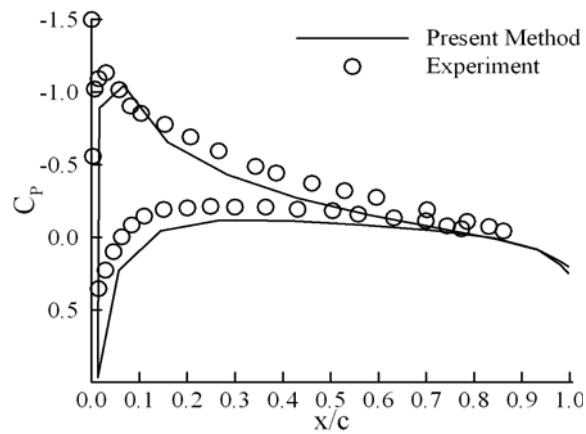Figure 4: Wake geometry in the hovering with 1-blade

Figure 5: Pressure distribution of the 1-blade in the hovering

reasonable shape of wake. This numerical method was compared with experimental results and theoretical results. Most results were satisfied to predict in various cases. Therefore, it will be able to offer the aerodynamic characteristics to rotary aircraft engineer through amount of prompt gathering aerodynamic data. With large amount of aerodynamic data, the performances of rotor can be predicted and it is supposed to set the up-to-date environment for design of rotary wing aircraft. The
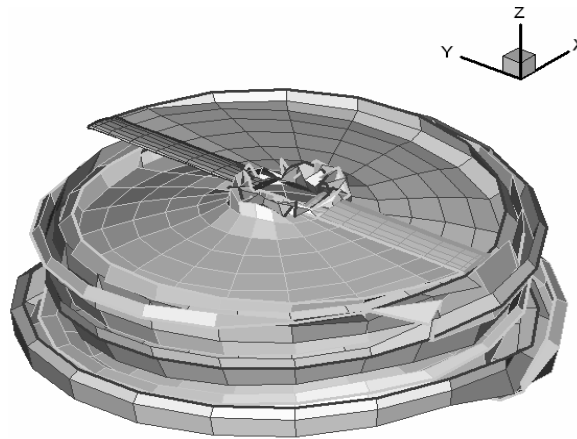
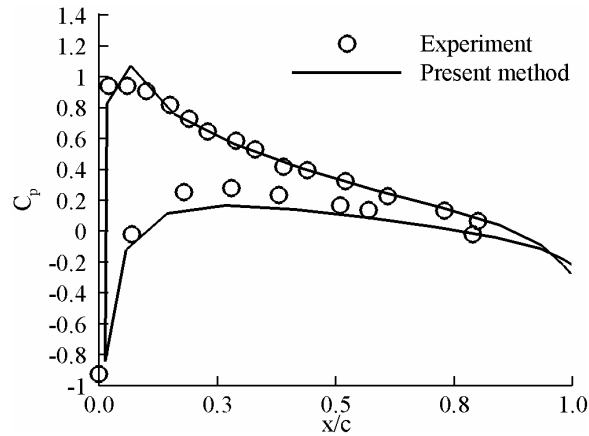Figure 6: Wake geometry of 2-blade in the hovering

Figure 7: Pressure distribution of the 2-blades in the hovering

present method is considerably efficient in terms of computing efforts as well as costs and offers great versatility in the aerodynamic design of the KHP and flight simulations.

In order to be able to determine blade lift, drag and flapping moment, and, ultimately, rotor performance, it is necessary, as with axial flight, to determine the induced velocity in forward flight. To compute more complicated rotor blade such as UH-60a, various cases of complex geometry have to be analyzed with amount of results of experiments.

Acknowledgement

References

1. Pengfei Liu, "A Time-Domain Panel Method for Oscillating Propulsor with Both Chordwise and Spanwise Flexibility," *Ph. D. Thesis, Faculty of Engineering & Applied Science*, Memorial University of Newfourd St. John's, 1996.

2. Moran, J., *Theoretical and Computational Aerodynmics*, John Wiley & Sons, New York, 1984.

3. Hess, J.L., "Calculation of Potential Flow about Arbitrary Three-Dimensional Lifting Bodies," *Final Technical Report, McDonnel Douglas Report No. MOC J5679-01*, Oct., 1972.

4. Caradonna, F. X., and Tung, C., "Experimental and Analytical Studies of a Model Helicopter Rotor in Hover," NASA TM-81232, 1981.

5. George Done and David Balmford., *Bramwell's Helicopter dynamics,* Butterworth Heinemann, Oxford, 2001.

6. Hess, J.L., "Calculation of Potential Flow about Arbitrary Three-Dimensional Lifting Bodies," *Final Technical Report, McDonnell Douglas Report No. MOC J5679-01*, Oct. 1972.

7. Maskew, B., VSAERO User's Manual (Revision E.5), Analytical Methods, Inc., Apr. 1994.

8. Katz, J. and Plotkin, A., *Low-Speed Aerodynamics*, 2nd Ed., Cambridge University Press, New York, 2001.